ELSEVIER

Microelectronic Engineering 46 (1999) 223–226

MICROELECTRONIC ENGINEERING

SCALPEL Mask-Membrane Charging

M. Mkrtchyan, A. Gasparyan, K. Mkhoyan, A. Liddle, A. Novembre, and D. Muller

Lucent Technologies, Bell Laboratories, Murray Hill, New Jersey 07974

Electrostatic charge generation and accumulation in a:SiN_x thin films irradiated by energetic (100 keV) electrons is investigated and kinetic equations describing the dynamic process are formulated. It is found that the incident electrons, inelastically scattered in the membrane, primarily generate plasmons. The plasmon decay creates electron-hole pairs and secondary electrons (SE). The escape of the SEs from the target leads to a positive electrostatic charge accumulation in the membrane. It is shown that SCALPEL® mask-membrane charging is defined by the balance of the SE escape, hole trapping and transport processes.

1. INTRODUCTION

Charging of the SCALPEL mask-membranes can have an adverse effect on the system performance. Charging creates an electrostatic field in the membrane that deflects the incident beam electrons while they travel through the mask-membrane. In order to ensure that the effect is within acceptable limits, we must first understand how charging occurs, and what effects it has on the final image.

Currently, SCALPEL masks comprise a SiN_x thin film supported by a massive Silicon grillage.[1] The latter can be grounded to provide a conductive path for the electrostatic charge accumulated in the film during the irradiation by the energetic electrons. Nevertheless, one cannot expect effective transport of the accumulated electrostatic charge due to the limited conductivity of the dielectric membrane material, the small cross-section of the conductive path (the membrane thickness ranges from 750 Å to 1500 Å), and the existence of high density trapping centers of the charge carriers. Because the trapping centers are uniformly distributed throughout the membrane, the charge accumulated in the membrane will be distributed uniformly as well, giving rise to a non-uniform distribution of the electrostatic field, $\boldsymbol{E}$, in the sub-field: $\boldsymbol{E}$ will be zero in the center and maximal at the edge of the sub-field. Depending on the exposure dose, the electrostatic field will cause either image placement error in the wafer (for low doses) or non-uniform distribution of the illumination at the wafer across the scan stripe[1] (for high doses).

In the case of an insulating film constantly irradiated by energetic electrons, continuous charging of the film will be terminated when the positive surface potential created by the accumulated electrostatic charge is strong enough to prevent the escape of the low energy secondary electrons from the film.[2,3] In the case of dielectric films with the limited conductivity, charging will be governed, in principle, by both the transport of charge carriers and the surface potential build up. In the SiN_x thin films considered here, the dielectric conductivity, though limited, is sufficient to limit the potential build up to less than 1 V; this potential locks only the low energy secondary electrons.

The film charging effect is sensitive to many factors such as the material electrical characteristics, its electronic structure and the sample geometry. For instance, film thickness change might change not only the quantity but also the sign of the accumulated charge and related surface potential.[3] In this paper we analyze the mechanism of charging of free standing dielectric films and develop a model of the charging of SiN_x membranes exposed to high energy (E = 100 keV) electrons. This model gives us (i) a realistic estimate of this effect and (ii) helps to find an effective way of eliminating the adverse effects of the membrane charging.

2. INCIDENT ELECTRON ENERGY LOSSES

The primary mechanisms of electron energy loss, caused by inelastic scattering, are the generation of plasmons (collective oscillations of the valence band electrons), ionization of a target atom and core electron excitation accompanied by X-ray or Auger-electron production. Depending on the target thickness (for given E) different mechanisms of electron losses become dominant.[1]

This work was partially supported by DARPA and SEMATECH

0167-9317/99/$ – see front matter
PII: S0167-9317(99)00067-2

2.1. Plasmon Losses

In thin Al films of thickness, t_m, comparable with the plasmon generation mean free path, Λ_p, the transmission electron energy loss spectra (EELS) show[2,4,5] that a large fraction of electrons passes through the film without energy loss (only elastic scattering). The only noticeable losses correspond to the energy losses of multiples of the plasmon energy, E_p; peak intensities decrease rapidly with the number of plasmons. At medium thicknesses (Ref. 4, Fig. 5.29), several plasmon loss-peaks are superimposed on a broad maximum due to overlapping of the L-ionization edge and the plasmon losses.

That plasmon losses are dominant in thin films has been conformed by our experimental studies of SiN_x membranes using EELS. Fig. 1 shows a Lorentzian shape for the 1st plasmon loss spectrum with the maximum at $E_p \approx 23.5$ eV and the width $\Delta E_p \approx 10.5$ eV. The mean-free-path of plasmon generation, $\Lambda_p = (\sigma_p N_e)^{-1}$, is related to the interaction cross section, σ_p, and the density of electrons in the valence band, N_e. For completely free electrons ($\Delta E_p \rightarrow 0$), both dielectric theory and quantum mechanics give $\Lambda_p = (a_H/\theta_E)/ln(\theta_c/\theta_E) \approx 100nm$, where a_H is the Bohr radius, $\theta_E \approx E_p/2E$, $\theta_c \approx E_p/(4EE_F)^{1/2}$, and E_F (≈ 18 eV for SiN_x) is the Fermi energy.[5] In reality, the valence electrons are not completely free and suffer energy losses due to their interaction with the ion cores.[5] The latter leads to finite ΔE_p (Fig. 1) and will increase Λ_p by a factor of 1.15 in the case of SiN_x.

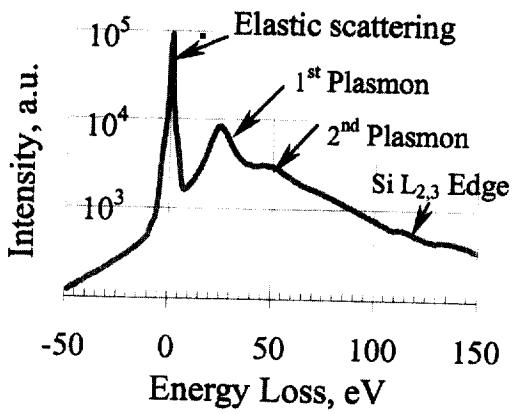

Fig. 1. EELS of 100 keV electrons incident on 120 nm SiN_x (collection semi-angle = 16 mrad, beam convergence semi-angle = 10 mrad)

2.2. Ionization Losses

The components of SiN_x have the following electronic structures; Si has K, L, M-shell electrons ($1s^2 2s^2 2p^6 3s^2 3p^2$), while N has only K and L-shell electrons ($1s^2 2s^2 2p^3$). In this case, the outer-shell electrons of each component, M-shell electrons of Si and L-shell electrons of N, compose the valence band electron gas that responds to an incident fast electron in the form of collective plasma oscillations (Sec. 2.1). Therefore, the remaining K-shell electrons of both components and L-shell electrons of Si ($2s^2 2p^4$) will contribute to the ionization of SiN_x.

The classical theory of electron inelastic scattering on an atom developed by Grysinski has been used to calculate partial ionization cross sections for the individual atomic shells:[6] $\sigma_{k\text{-}x} = \sigma_0 Z_{k\text{-}x} g_{k\text{-}x}(y)$, where $\sigma_0 = (e^4/16\pi\varepsilon_0 U_{k\text{-}x}^2)$, ε_0 is the permittivity of the free space, $Z_{k\text{-}x}$ and $U_{k\text{-}x}$ are the number of electrons and the average ionization energy in the sub-shell denoted by k-x (k = K, L, M etc., and x = 1s, 2s, 2p, etc), $y = E_0/U_{k\text{-}x}$, and $g_{k\text{-}x}(y)$ is a function given by Eq. 22 of Ref. 6. Using $Z_{L\text{-}2s} = 2$, $Z_{L\text{-}2p} = 6$, $U_{K\text{-}1s} \approx 1500$ eV, $U_{L\text{-}2s} \approx 150$ eV (both for Si), and $U_{L\text{-}2p} \approx 113$ eV, we found $\sigma_L^{Si} = \sigma_{L\text{-}2s}^{Si} + \sigma_{L\text{-}2p}^{Si} \approx 1.25\sigma_{L\text{-}2p}^{Si} = 1.4 \cdot 10^{-19} cm^2$ for $E = 100$ keV. The mean free path corresponding to L-shell ionization is defined by the number of Si atoms per unit volume in SiN_x; for a silicon rich silicon nitride $N_{Si} \approx 0.5 N_{SiNx} = 4.4 \cdot 10^{22}$ cm^{-3}: $\Lambda_{ion.L}^{Si} = [N_{si}\,\sigma_L^{Si}]^{-1} \approx [0.5\, N_{SiNx}\,\sigma_L^{Si}]^{-1} \approx 1600$ nm. This result correlates well with the measured EELS of amorphous SiN_x (Fig. 1) which displays a significant difference between the EELS intensities at 1st plasmon loss energy and at the $L_{2,3}$-edge of Si; the ratio of corresponding peaks is approximately equal to the ratio $\Lambda_p/\Lambda_{ion.L}^{Si} \approx 0.1$.

3. SE EMISSION AND ELECTRON-HOLE PAIR GENERATION

The total number of SE is related to the number of secondary electrons, dN/dE_1, yielded in the energy interval E_1, E_1+dE_1 as follows:[2]

$$\delta = \int_{W}^{W+E_{B0}} \{dN/dE_1\} dE_1 ,$$

$$dN/dE_1 = \int_0^{\alpha_0} \int_0^{t_m} F(E_1,E_0,z)\, exp[-z/\Lambda(E_1)\, cos\alpha]\, d\alpha\, dz.$$

Here W is the minimum energy that an electron needs to overcome the material work function, α_0 is the critical angle for total internal reflection of a SE obtained from the condition $cos^2\alpha_0 = W/E_1$,[2]

$F(E_1,E,z)$ is the number of electrons excited in the energy interval E_1,E_1+dE_1 at the depth z (Ref. 7, Eq. 14), and $\Lambda(E_1)$ is the *total* mean free path of inelastic scattering of an electron of energy E_1 (Ref. 8, Eq. 14), E_{B0} is the upper edge of SE distribution (~50 eV)[2]. Because the plasmon losses are dominant, $\Lambda_{ion} >> \Lambda_p$, valence electrons are excited above the bottom of the conduction band mostly due to the decay of plasmons. Therefore, the generation of SEs will occur in a relatively small volume and the calculation procedure can be simplified by assuming that the function $F(E_1,E,z)$ does not depend on z. This function can be also used to calculate the rate of electron-hole pair generation as follows:

$$g = (I \cdot g_1),\ g_1 = (eV)^{-1}\left[t_m \int_{E_F+E_G}^{W+E_{B0}} F(E_1,E_0)dE_1 - \delta\right]$$

where I is the beam current, V is the membrane volume exposed to the beam. For the case t_m=120 nm, sub-field area a^2=1x1 mm^2 ($V=a^2 \cdot t_m \approx 1.2\ 10^{-13}$ m^3) we have found $\delta \approx 1.5 \cdot 10^{-4}$ and $g_1 \approx 6 \cdot 10^{29}$ m^{-3}s^{-1}.

4. CHARGING MECHANISM AND KINETIC EQUATIONS

The process of the charging of a dielectric membrane irradiated by a flux of energetic electrons can be described on the basis of a simplified schematic of energetic states shown in Fig. 2. The

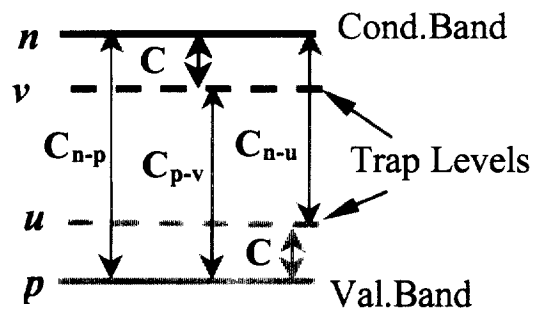

Fig.2. Energetic states of mobile and trapped charge carriers with the population densities shown on the left.

incident electron beam creates electrons and holes that are then transported, recombine, or get captured by the trap centers - the majority are eventually localized at the trap levels situated in the gap. Some mobile electrons escape from the membrane surfaces as SEs giving rise to a positive membrane charge; as a consequence, *only hole transport* in the dielectric is expected. The kinetics for the population of the four states shown in Fig. 2 can then be described by the following set of equations:

$$dn/dt = g_1 I - Cn(\nu_m - \nu) - C_{n\text{-}p} np - C_{n\text{-}u} nu \quad (1)$$

$$dp/dt = g_1 I + \delta I/(eV) - C_{p\text{-}v} pv - C_{n\text{-}p} np - Cp(u_m - u) - (\zeta/eV)\mu_h(p+\chi N_{t\text{-}N})(p+u-\nu-n), \quad (2)$$

$$du/dt = Cp(u_m - u) - C_{n\text{-}u} nu, \quad (3)$$

$$dv/dt = Cn(\nu_m - \nu) - C_{p\text{-}v} pv. \quad (4)$$

where $\zeta \approx 4 \cdot 10^{-27} a t_m^2 (1+\varepsilon)^{-1}$ is a measure of electrostatic field strength of the net charge, $q(t)= e[p(t)+u(t)-\nu(t)-n(t)]$, accumulated in the exposed region of the membrane [ζ regulates the hole flux, $I_h = \zeta\mu_h(p+\chi N_{t\text{-}N})q$], e is the electronic charge, ε is the membrane relative dielectric constant, μ_h is the hole drift mobility, ν_m and u_m are the maximum density of states available for electron and hole trapping, C is the capture rate of a free charge carrier by a charged trap center of opposite sign (the same value ($2.5 \cdot 10^{-12}$ m^3/s)[9] is used for electrons and holes). Here we have separated the direct electron-hole recombination (with the coefficient $C_{n\text{-}p}$) from their indirect recombination through the trap levels (with the coefficients $C_{n\text{-}u}$ and $C_{p\text{-}v}$ for mobile electrons and holes correspondingly). This enables us to describe the evolution of the population of all the states involved, though in the reality it is difficult to design an experiment to distinguish these three processes.[10] There are no experimental data for these coefficients in the case of amorphous SiN_x. Here we use $C_{n\text{-}u} \approx 2 \cdot 10^{-17}$ m^3/s and $C_{p\text{-}v} \approx C_{n\text{-}p} \approx 1.0 \cdot 10^{-17}$ m^3/s that seems to be in a range seen in other amorphous insulators and were chosen to give good fit of the results of an accurate simulation of the inerfacial charge build-up in MNOS devices under irradiation with the corresponding experimental data.[10]

The last term in Eq. 2 describes hole transport in the sample. It accounts for the fact that the shallow hole trap levels related to the N-dangling bonds are situated very close to the valence band[11] and a fraction of holes, $\chi N_{t\text{-}N}$, trapped at the levels with $E_t \leq kT \approx 0.02$ eV (k is the Boltzman constant and $T \approx 300$ K) will directly contribute to the hole conductivity due to their thermal release into the valence band (hopping conductivity).[12] The shallow trap levels' distribution has a maximum at $E_{tm} \approx 0.2$ eV.[11] Assuming that they are distributed according to the Boltzman distribution, we have found $\chi \approx 10^{-4}$.

In Eqs. 1-4 we account for the capture of mobile charge carriers only by charged trap centers because the measured cross section of this process, $\sigma_{+cap} \approx 2.88 \rightarrow 5.0 \cdot 10^{-13}$ cm^2, is about two orders of magnitude

larger than the cross section for electron trapping on a neutral trap center.[9,13]

Combining Eqs 1-4 one can see that the electrostatic charge accumulation is described by the equation:

$$dq(t)/dt = \delta \cdot I/(V) - \mu_h(\zeta/eV)(p(t) + \chi N_{t\text{-}N})q(t). \quad (5)$$

In general, δ is an indirect function of the time, $\delta=\delta(q(t))$, due to the surface potential built up by the accumulated electrostatic charge. In the first approximation one can assume δ constant and from Eq. 5 we can find the steady state density of the charge accumulated in the membrane: $q_0 = e\delta I_p/[\zeta\mu_h(p_0 + \chi N_{t\text{-}N})]$. The exact numerical solution of the system of Eqs. 1-4 shows that $p_0 << \chi N_{t\text{-}N}$ (a consequence of the fast hole capture on trap levels) and, therefore, $q_0 \approx e\delta I_p/(\zeta\mu_h\chi N_{t\text{-}N})$, where $N_{t\text{-}N} \leq 0.25\cdot10^{24}$ m^{-3}.[14]

Exploiting $p(t) << \chi N_{t\text{-}N}$, we find from Eq. 5 an exponential time evolution of the charging in thin SiN_x membranes, $q(t) = q_0[1 - exp(-t/\tau)]$, with a characteristic time constant $\tau = [(\mu_h\zeta\chi N_{t\text{-}N})/(eV)]^{-1}$.

5. SIMULATION RESULTS AND DISCUSSION

An example of an exact numerical solution of Eqs. 1-4 for the case of a 120 nm a-$SiN_{0.5}$ membrane with $\mu_h \approx 5\cdot10^{-6}$ m^2/(Vs), are shown in Fig. 3; one can see that the membrane charging rate is independent of the beam current, while the steady state charge increases proportional to the beam current; these results agree well with our analytical findings for τ and q_0.

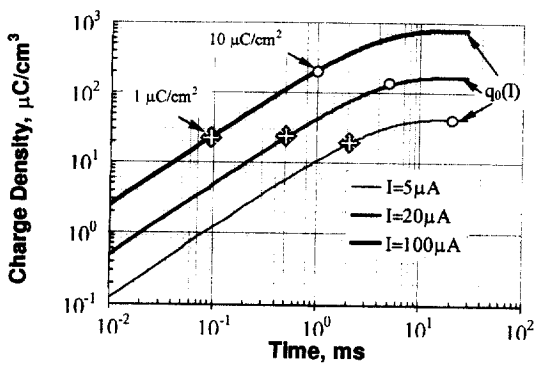

Fig.3. Accumulated charge density vs the exposure time calculated for different beam currents: circles and crosses correspond to the accumulated charge when low and high sensitivity resists are exposed. The higher the resist sensitivity, the less the importance of charging.

We have simulated the process using μ_h ranging from $5\cdot10^{-8}$ to $5\cdot10^{-6}$ m^2/(Vs), (possibly highest mobility for an a-SiN_x) to find the sensitivity of the membrane charging to this parameter. We have found that both the transient time, Δt, and q_0 are $\propto\mu_h^{-1}$ that correlates with the expressions for τ and q_0 obtained analytically (Sec. 4).

SCALPEL membrane charging will deflect the trajectories of incident electrons. Our analysis shows that (i) if the deflection angle, $\alpha(q)$, is smaller than the SCALPEL aperture angular size, α_0,[1] the membrane charging will cause a pattern placement error that ranges from 0 (at the center of the sub-field) to a maximum value, Δx_{max} (at the edge of the sub-field); (ii) if $\alpha > \alpha_0$, there is expected illumination intensity lost at the sub-field edge (details to appear in the future publications). For a SCALPEL tool operating with the beam current I = 100 μA incident on the 120 nm SiN_x mask-membrane, we have found: $\alpha(q) \approx 4.5\cdot10^{-6}q$ and $\Delta x_{max} \approx 5.5\cdot10^{-4}\alpha(q)$; if a resist of 5 μC/cm^2 sensitivity is used, $\Delta x_{max} \approx 25$ nm.

Our results demonstrate that the membrane charging is sensitive to both the conductivity and the geometry of the conductive path, and, therefore, can be regulated by tailoring both of them.

REFERENCES

1. L. R. Harriott et al., Microelectron. Eng., **35**, (1997) 477.
2. L. Reimer, *Scanning Electron Microscopy. Physics of Image Formation and Microanalysis*, Springer-Verlag, Berlin, 1989.
3. W. Liu, J. Ingino, and R. F. Pease, J. Vac. Sci. Techn., B **13**, (1995) 1979
4. L. Reimer, *Transmission Electron Microscopy. Physics of Image Formation and Microanalysis*, Springer-Verlag, Berlin, 1989.
5. R. F. Egerton, *Electron Energy-Loss Spectroscopy in The Electron Microscopy*, Plenum Press, New York, 1996.
6. M. Grisinsky, Phys. Rev., **138**, (1965) A336.
7. H. W. Streitwolf, Ann. Physik, **3**, (1959) 183.
8. J. Quinn, Phys. Rev. **126**, (1962) 1453.
9. K. Lehovec and D. W. Crain, J. Appl. Phys., **47**, (1976) 2763.
10. R. C. Hughes, Proc. of The Symp. on *Silicon Nitride Thin Insulating Films*, (1983) 235.
11. J. Robertson, Philos. Mag. B, **63**, (1991) 47.
12. S. Fujita, A.Sasaki, J.Electrochem.Soc. **132**, (1985) 398
13. P. Arnett, B. Yun, Appl.Phys.Lett. **26**, (1975) 94.
14. V. Kapoor, R.Turi, J.Appl. Phys. **52**, (1981) 311.